

CBBN in the CMSSM

J. Pradler^a, F.D. Steffen

Max-Planck-Institut für Physik, Föhringer Ring 6, 80805 Munich, Germany

Received: 16 February 2008 / Revised version: 23 May 2008 /

Published online: 8 July 2008 – © Springer-Verlag / Società Italiana di Fisica 2008

Abstract. Catalyzed big bang nucleosynthesis (CBBN) can lead to overproduction of ${}^6\text{Li}$ in gravitino dark matter scenarios in which the lighter stau is the lightest standard model superpartner. Based on a treatment using the state-of-the-art result for the catalyzed ${}^6\text{Li}$ production cross section, we update the resulting constraint within the framework of the constrained minimal supersymmetric standard model (CMSSM). We confront our numerical findings with recently derived limits on the gaugino mass parameter $m_{1/2}$ and the reheating temperature T_R .

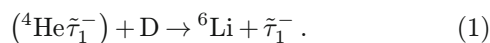
PACS. 12.60.Jv; 95.35.+d

1 Introduction

Big bang nucleosynthesis (BBN) is a cornerstone of modern cosmology that allows us to probe physics beyond the standard model. It has been realized recently that the presence of massive long-lived negatively charged particles X^- at the time of BBN can have substantial impact on the primordial light element abundances via bound-state formation [1–11].

In scenarios in which the gravitino \tilde{G} is the lightest supersymmetric particle (LSP), a long-lived X^- may be realized if the lighter stau $\tilde{\tau}_1$ is the next-to-lightest supersymmetric particle (NLSP). In particular, a $\tilde{\tau}_1$ NLSP can be accommodated naturally in the framework of the constrained minimal supersymmetric standard model (CMSSM) [4, 12–15] in which the gaugino masses, the scalar masses, and the trilinear scalar couplings are assumed to take on the respective universal values $m_{1/2}$, m_0 , and A_0 at $m_{\text{GUT}} \simeq 2 \times 10^{16}$ GeV. There the stau emerges as the lightest standard model superpartner in a large part of the CMSSM parameter space. Since the couplings of the stau to the gravitino are suppressed by the (reduced) Planck scale, $M_{\text{P}} = 2.4 \times 10^{18}$ GeV, $\tilde{\tau}_1$ will typically be long-lived for conserved R -parity¹ and thus $\tilde{\tau}_1^- = X^-$.

Then $\tilde{\tau}_1^-$ and ${}^4\text{He}$ can form bound states, (${}^4\text{He}\tilde{\tau}_1^-$), and too much ${}^6\text{Li}$ can be produced via the catalyzed (CBBN) reaction [1]



This happens at temperatures $T \simeq 10$ keV [1] when standard BBN (SBBN) processes are frozen out. The observationally inferred bound on primordial ${}^6\text{Li}$ then severely

restricts the $\tilde{\tau}_1$ abundance at those times² and thereby the $\tilde{\tau}_1$ lifetime $\tau_{\tilde{\tau}_1}$.

For conserved R -parity, the gravitino LSP is stable and is a promising dark matter candidate. After inflation, gravitinos are regenerated [18] in thermal scattering of particles in the primordial plasma. The resulting gravitino density $\Omega_{\tilde{G}}^{\text{TP}}$ will contribute substantially to the dark matter density Ω_{dm} if the radiation-dominated epoch starts with a high reheating temperature T_R [19–21]. In addition, gravitinos are produced in stau NLSP decays with the respective density $\Omega_{\tilde{G}}^{\text{NTP}}$ [12, 22, 23].³

In this work we study gravitino dark matter scenarios within the framework of the CMSSM in which $\tilde{\tau}_1$ is the NLSP. For two exemplary parameter scans, we compute $\Omega_{\tilde{G}} = \Omega_{\tilde{G}}^{\text{TP}} + \Omega_{\tilde{G}}^{\text{NTP}}$ at every point in the associated $(m_0, m_{1/2})$ planes and compare it with Ω_{dm} . Regions with $\Omega_{\tilde{G}} = \Omega_{\text{dm}}$ are shown and their shape is discussed. The $\tau_{\tilde{\tau}_1}$ -dependent exclusion boundary on the stau abundance from ${}^6\text{Li}$ overproduction allows us to infer cosmologically disfavored CMSSM regions. Our numerical findings are confronted with the recently derived analytic expressions for limits on $m_{1/2}$ and T_R [11]. To illustrate potentially severe implications for phenomenology at the Large Hadron Collider (LHC), the gluino mass contour $m_{\tilde{g}} = 2.5$ TeV is indicated for exemplary CMSSM scenarios. Additional BBN constraints from the primordial abundances of D and ${}^3\text{He}$ are shown. We discuss the present status of the relevant BBN constraints at the end of Sect. 4.

² In this work we assume a standard cosmological history in which $\tilde{\tau}_1$ was in thermal equilibrium before decoupling.

³ We do not include gravitino production from inflaton decays; cf., e.g., [24, 25] and references therein.

^a e-mail: jpradler@mppmu.mpg.de

¹ For the case of broken R -parity, see, e.g., [16, 17].

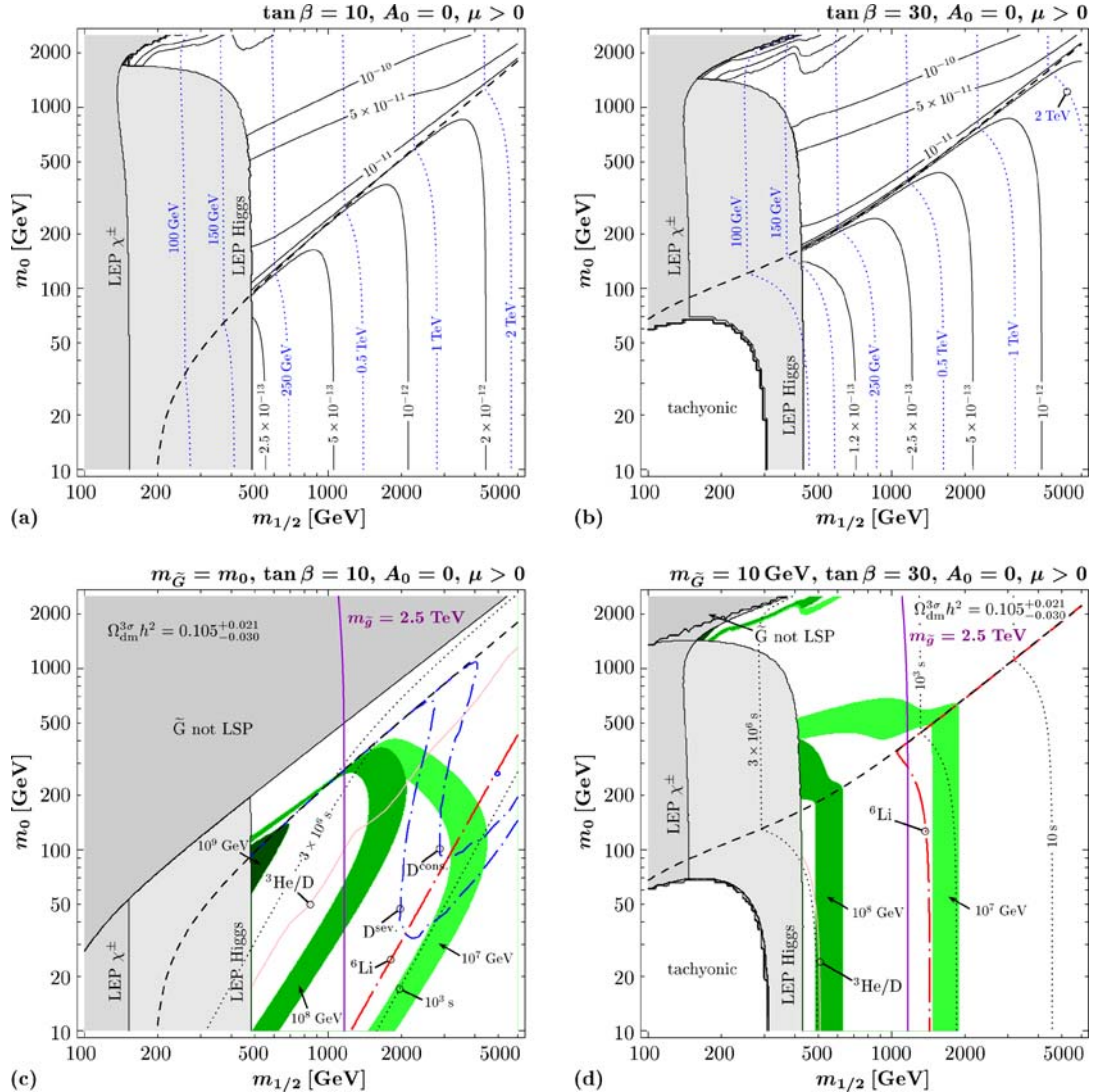


Fig. 1. The $(m_{1/2}, m_0)$ planes for $A_0 = 0, \mu > 0$, and the choices **a,c** $\tan \beta = 10$ and **b,d** $\tan \beta = 30$. Above (below) the *dashed lines*, $m_{\tilde{\chi}_1^0} < m_{\tilde{\tau}_1}$ ($m_{\tilde{\tau}_1} < m_{\tilde{\chi}_1^0}$). The *medium gray* and the *light gray* regions at small $m_{1/2}$ are excluded respectively by chargino and Higgs searches at LEP. In the upper panels, contours of $Y_{\text{NLSP}}^{\text{dec}}$ (*solid*) and m_{NLSP} (*dotted*) are shown. In the associated lower panels, we consider scenarios with **c** $m_{\tilde{G}} = m_0$ and **d** $m_{\tilde{G}} = 10$ GeV. The *light, medium, and dark shaded (green in the web version) bands* indicate the regions in which $0.075 \leq \Omega_{\tilde{G}} h^2 \leq 0.126$ for $T_R = 10^7, 10^8$, and 10^9 GeV, respectively. In the dark gray region, the gravitino is not the LSP. The *dotted lines* show contours of the NLSP lifetime. With the $\tilde{\tau}_1$ NLSP, the region to the left of the *long-dash-dotted (red in the web version) line* is disfavored by the primordial ${}^6\text{Li}$ abundance. Constraints from primordial D disfavor the $\tilde{\tau}_1$ NLSP region above the *short-dash-dotted lines*. The region to the left of the *thin gray (pink in the web version) line* is disfavored by ${}^3\text{He}/\text{D}$ [30]. On the *solid vertical (violet in the web version) line* $m_{\tilde{g}} = 2.5$ TeV

2 Gravitino dark matter in the CMSSM

In the CMSSM, the superparticle mass spectrum is determined by specifying $m_0, m_{1/2}, A_0$, the ratio of the two MSSM Higgs doublet vacuum expectation values, $\tan \beta$, and the sign of the higgsino mass parameter μ . Then either the lightest neutralino $\tilde{\chi}_1^0$ or the lighter stau $\tilde{\tau}_1$ with respective masses $m_{\tilde{\tau}_1}$ and $m_{\tilde{\chi}_1^0}$ is the lightest standard model superpartner and hence the NLSP⁴, whose mass is denoted by m_{NLSP} .

⁴ A stop \tilde{t}_1 NLSP is not feasible in the CMSSM [26].

With the gravitino LSP, the relic density from NLSP decays reads

$$\Omega_{\tilde{G}}^{\text{NTP}} h^2 = m_{\tilde{G}} Y_{\text{NLSP}}^{\text{dec}} s(T_0) h^2 / \rho_c, \quad (2)$$

where $m_{\tilde{G}}$ is the gravitino mass. The quantity $Y_{\text{NLSP}}^{\text{dec}} = n_{\text{NLSP}}^{\text{dec}}/s$ denotes the NLSP yield where $n_{\text{NLSP}}^{\text{dec}}$ is the number density at decoupling and $s = 2\pi^2 g_* s T^3/45$ the entropy density; $\rho_c/[s(T_0)h^2] = 3.6 \times 10^{-9}$ GeV [27]. We obtain $Y_{\text{NLSP}}^{\text{dec}}$ by employing the computer program micrOMEGAs 1.3.7 [28, 29], which we feed with the

superparticle mass spectrum computed with SuSpect 2.34.⁵

The upper panels in Fig. 1 show the contours of $Y_{\text{NLSP}}^{\text{dec}}$ (solid) and m_{NLSP} (dotted) in the $(m_{1/2}, m_0)$ plane for $A_0 = 0$, $\mu > 0$, (a) $\tan\beta = 10$ and (b) $\tan\beta = 30$. Above (below) the dashed line, $m_{\tilde{\chi}_1^0} < m_{\tilde{\tau}_1}$ ($m_{\tilde{\tau}_1} < m_{\tilde{\chi}_1^0}$). The medium gray and the light gray regions at small $m_{1/2}$ are excluded respectively by the mass bounds $m_{\tilde{\chi}_1^\pm} > 94 \text{ GeV}$ and $m_h > 114.4 \text{ GeV}$ from chargino and Higgs searches at LEP [27]. For $\tan\beta = 30$, tachyonic fermions occur at points in the white corner labeled as “tachyonic”.

Let us now explore the parameter space in which the relic gravitino density matches the observed dark matter density [27] $\Omega_{\text{dm}}^{3\sigma} h^2 = 0.105_{-0.030}^{+0.021}$, where h is the Hubble constant in units of $100 \text{ km Mpc}^{-1} \text{ s}^{-1}$. Then T_{R} and $m_{\tilde{G}}$ appear in addition to the CMSSM parameters. In the lower panels of Fig. 1, the shaded bands (green in the web version) are the $(m_{1/2}, m_0)$ regions in which

$$0.075 \leq \Omega_{\tilde{G}}^{\text{TP}} h^2 + \Omega_{\tilde{G}}^{\text{NTP}} h^2 \leq 0.126 \quad (3)$$

for the indicated values of T_{R} and for (c) $m_{\tilde{G}} = m_0$ and (d) $m_{\tilde{G}} = 10 \text{ GeV}$. For $\Omega_{\tilde{G}}^{\text{TP}}$, we use (3) of [20]⁶, while $\Omega_{\tilde{G}}^{\text{NTP}}$ is computed as explained above. In the dark shaded regions at larger m_0 , the gravitino is not the LSP.

3 Catalyzed BBN of ${}^6\text{Li}$ in the CMSSM

We now focus on the $\tilde{\tau}_1$ NLSP region. For typical values of $Y_{\tilde{\tau}_1}^{\text{dec}} = Y_{\text{NLSP}}^{\text{dec}}/2$ (see Fig. 1a and b), the amount of ${}^6\text{Li}$ produced in the CBBN reaction (1) can be as high as ${}^6\text{Li}/\text{H}|_{\text{CBBN}} = 10^{-7}$ [1, 5, 11] and hence can be far in excess of the observationally inferred upper limit on the primordial ${}^6\text{Li}$ abundance [31]

$${}^6\text{Li}/\text{H}|_{\text{obs}} \lesssim 2 \times 10^{-11}. \quad (4)$$

For $\tau_{\tilde{\tau}_1} \lesssim 5 \times 10^3 \text{ s}$ [1, 5, 6, 8, 11], however, the staus decay before (1) becomes too efficient so that ${}^6\text{Li}/\text{H}|_{\text{CBBN}}$ can be in agreement with (4). From the $\tau_{\tilde{\tau}_1}$ -dependent upper limit on $Y_{\tilde{\tau}_1}^{\text{dec}}$ computed in [11] by solving the Boltzmann equations containing the state-of-the-art result for the catalyzed ${}^6\text{Li}$ production cross section [5], we obtain the long-dash-dotted lines in the lower panels of Fig. 1. The regions to the left of these lines are cosmologically disfavored because of overproduction of ${}^6\text{Li}$.⁷ Note that only the constraint from the primordial D abundance on hadronic energy release [30, 32] in $\tilde{\tau}_1$ decays [13, 23, 33] can

be more severe than the one from catalyzed ${}^6\text{Li}$ production [4, 7, 15, 34].⁸ This is shown by the short-dash-dotted lines in panel c, which exclude the region in the $\tilde{\tau}_1$ NLSP region above these lines. In panel d the D constraint does not appear; for details on this constraint see [15, 33]. Contours of the NLSP lifetime are shown by the dotted lines.

4 Discussion

The position of the ${}^6\text{Li}$ constraint is governed by the stau lifetime. From the constraint $\tau_{\tilde{\tau}_1} \leq 5 \times 10^3 \text{ s}$, limits on the gaugino mass parameter,

$$m_{1/2} \geq 0.9 \text{ TeV} \left(\frac{m_{\tilde{G}}}{10 \text{ GeV}} \right)^{2/5}, \quad (5)$$

and the reheating temperature,

$$T_{\text{R}} \leq 4.9 \times 10^7 \text{ GeV} \left(\frac{m_{\tilde{G}}}{10 \text{ GeV}} \right)^{1/5} \quad (6)$$

have been derived recently [11] for a typical yield $Y_{\tilde{\tau}_1}^{\text{dec}} \gtrsim 3.5 \times 10^{-14} (m_{\tilde{\tau}_1}/100 \text{ GeV})$ [22]. Note that these limits, obtained in the framework of the CMSSM, do only depend on $m_{\tilde{G}}$.

The limit (5) emerges since $m_{\tilde{\tau}_1}$ scales with $m_{1/2}$ (see Fig. 1a and b) and since $\tau_{\tilde{\tau}_1}$ is fixed once $m_{\tilde{G}}$ and $m_{\tilde{\tau}_1}$ are specified. The choice $m_{\tilde{G}} = 10 \text{ GeV}$ in Fig. 1d allows for an immediate comparison of our numerical findings with (5) and (6). Only in the vicinity of the dashed line, i.e., in the $\tilde{\tau}_1\text{-}\tilde{\chi}_1^0$ coannihilation region, the position of the ${}^6\text{Li}$ constraint approaches the lower limit (5). This is because $\tilde{\tau}_1$ becomes heavier for larger m_0 , which shortens $\tau_{\tilde{\tau}_1}$ for fixed $m_{\tilde{G}}$. Contrariwise, the splitting between the actual position of the ${}^6\text{Li}$ constraint and (5) is larger for smaller m_0 . At $m_0 = 10 \text{ GeV}$, this is more pronounced in Fig. 1d than in Fig. 1c. This results from the fact that the increase in $\tan\beta$ leads to a decrease in $m_{\tilde{\tau}_1}$, so that $\tau_{\tilde{\tau}_1}$ becomes larger for fixed $m_{\tilde{G}}$.

The limit (6) relies on thermal gravitino production only, $\Omega_{\tilde{G}}^{\text{TP}} \propto T_{\text{R}}$ [19–21]. Thus the upper limit on T_{R} can only become more stringent by taking $\Omega_{\tilde{G}}^{\text{NTP}}$ into account. In Fig. 1c we have fixed $m_{\tilde{G}} = m_0$. Thereby, non-thermal production (2) becomes more important for larger values of m_0 . In addition, $Y_{\tilde{\tau}_1}^{\text{dec}}$ takes on its maximum at a given $m_{1/2}$ in the $\tilde{\tau}_1\text{-}\tilde{\chi}_1^0$ coannihilation region. This leads to the bending of the bands (3) towards lower $m_{1/2}$. From Fig. 1c and d we thus find $T_{\text{R}} \lesssim 10^7 \text{ GeV}$ and we see that (6) provides a good conservative estimate for the shown scenarios. The bound $T_{\text{R}} \lesssim 10^7 \text{ GeV}$ can be very restrictive for models of inflation and baryogenesis.

Since for a $\tilde{\tau}_1$ NLSP typically $m_0^2 \ll m_{1/2}^2$, it is the gaugino mass parameter $m_{1/2}$ that sets the scale for the low energy superparticle spectrum. Thus, depending on $m_{\tilde{G}}$, the bound (5) implies high values of the superparticle masses

⁵ We use the following standard model parameters: $m_t = 172.5 \text{ GeV}$, $m_b(m_b)^{\overline{\text{MS}}} = 4.23 \text{ GeV}$, $\alpha_s^{\overline{\text{MS}}}(m_Z) = 0.1172$, and $\alpha_{\text{em}}^{-1\overline{\text{MS}}}(m_Z) = 127.90896$.

⁶ For the definition of T_{R} , see Sect. 2 in [15].

⁷ In this regard, cf. the discussion at the end of Sect. 4.

⁸ Additional constraints on the primordial light elements from CBBN can be found in [4, 6, 7, 10].

which can be associated with a mass range that will be difficult to probe at the LHC. This is illustrated by the vertical line (violet in the web version) in Fig. 1c and d which shows the gluino mass contour $m_{\tilde{g}} = 2.5$ TeV.⁹

In the above considerations we have assumed a standard thermal history of the universe during the radiation-dominated epoch. A substantial entropy release after the decoupling of the NLSP but before the onset of BBN may dilute and thereby reduce $Y_{\tilde{\tau}_1^-}^{\text{dec}}$ [35] such that ${}^6\text{Li}/\text{H}|_{\text{CBBN}}$ may respect the observationally inferred limit (4) even for long lifetimes, $\tau_{\tilde{\tau}_1^-} \gtrsim 5 \times 10^3$ s [5, 15]. The actual amount of entropy required, however, is model dependent. For example, if entropy is released by an out-of-equilibrium decay of a massive particle species ϕ , the presence of the energy density ρ_ϕ during NLSP decoupling enhances the Hubble rate. This would lead to an increase of the decoupling temperature and of the NLSP yield directly after decoupling. Furthermore, the branching ratio of the ϕ decays into $\tilde{\tau}_1$ and/or gravitinos may be substantial and may compensate part of the dilution of $Y_{\tilde{\tau}_1^-}^{\text{dec}}$; see, e.g., [24, 25].

An illustrative scenario taking into account the increased Hubble rate due to ρ_ϕ but assuming a negligible branching ratio of the ϕ decays into superparticles can be found in [15]. As argued in [36], however, a concrete realization of a large entropy release by ϕ decays in the narrow time window after NLSP decoupling and before BBN might be rather difficult to accomplish in the scenarios considered.

Let us finally comment on the present status of BBN constraints on gravitino dark matter scenarios with a long-lived charged slepton NLSP. In [10, 38] an elaborate CBBN study is carried out including additional late-time effects such as bound-state formation of X^- with protons at $T \simeq 1$ keV, i.e., for cosmic times $t \gtrsim 10^6$ s. By taking into account the uncertainties in the relevant nuclear reaction rates, it is shown explicitly in Fig. 14 in [10] and in Fig. 5 in [38] that the appearance of cosmologically allowed islands for $\tau_{\tilde{\tau}_1^-} \gtrsim 10^5$ s still remains very unlikely ($< 1\%$) with $Y_{\tilde{\tau}_1^-}^{\text{dec}} \gtrsim 3.5 \times 10^{-14} (m_{\tilde{\tau}_1^-}/100 \text{ GeV})$. In this region, the ${}^3\text{He}/\text{D}$ constraint on electromagnetic energy release [37] becomes severe and may exclude $\tau_{\tilde{\tau}_1^-} \gtrsim 10^6$ s [4, 7, 10, 13]. This is illustrated in Fig. 1c and d by the thin gray line which is obtained from Fig. 42 of [30] with a ‘visible’ electromagnetic energy of $E_{\text{vis}} = 0.3E_\tau$ of the tau energy $E_\tau = (m_{\tilde{\tau}_1^-}^2 - m_{\tilde{G}}^2 + m_\tau^2)/2m_{\tilde{\tau}_1^-}$ released in $\tilde{\tau}_1 \rightarrow \tilde{G}\tau$. Only with a finely tuned $m_{\tilde{\tau}_1^-} - m_{\tilde{G}}$ degeneracy leading to $E_{\text{vis}} \rightarrow 0$ can any bound on the energy release and in particular the one from ${}^3\text{He}/\text{D}$ be evaded.

5 Conclusion

We have considered gravitino dark matter scenarios in which $\tilde{\tau}_1$ is the NLSP. For exemplary CMSSM scenarios we have demonstrated that our recently obtained

limit [11] $T_{\text{R}} \leq 4.9 \times 10^7 \text{ GeV} (m_{\tilde{G}}/10 \text{ GeV})^{1/5}$ from catalyzed ${}^6\text{Li}$ production provides a good conservative estimate. In particular, taking into account $\Omega_{\tilde{G}}^{\text{NTP}}$, the T_{R} limit can become considerably more severe. While CMSSM phenomenology at the LHC could still be viable with a lighter gravitino, we have shown explicitly that the ${}^6\text{Li}$ constraint can exclude $m_{\tilde{g}} < 2.5$ TeV for $m_{\tilde{G}} \gtrsim 10$ GeV. For the natural gravitino LSP mass range in gravity-mediated supersymmetry breaking scenarios, the cosmologically favored region can thus be associated with a mass spectrum that will be very difficult to probe at the LHC.

References

1. M. Pospelov, Phys. Rev. Lett. **98**, 231 301 (2007)
2. K. Kohri, F. Takayama, Phys. Rev. D **76**, 063 507 (2007)
3. M. Kaplinghat, A. Rajaraman, Phys. Rev. D **74**, 103 004 (2006)
4. R.H. Cyburt, J.R. Ellis, B.D. Fields, K.A. Olive, V.C. Spanos, JCAP **0611**, 014 (2006)
5. K. Hamaguchi, T. Hatsuda, M. Kamimura, Y. Kino, T.T. Yanagida, Phys. Lett. B **650**, 268 (2007)
6. C. Bird, K. Koopmans, M. Pospelov, arXiv:hep-ph/0703096
7. M. Kawasaki, K. Kohri, T. Moroi, Phys. Lett. B **649**, 436 (2007)
8. F. Takayama, arXiv:0704.2785 [hep-ph]
9. T. Jittoh et al., Phys. Rev. D **76**, 125 023 (2007)
10. K. Jedamzik, Phys. Rev. D **77**, 063 524 (2008)
11. J. Pradler, F.D. Steffen, arXiv:0710.2213 [hep-ph]
12. J.R. Ellis, K.A. Olive, Y. Santoso, V.C. Spanos, Phys. Lett. B **588**, 7 (2004)
13. D.G. Cerdeno, K.Y. Choi, K. Jedamzik, L. Roszkowski, R. Ruiz de Austri, JCAP **0606**, 005 (2006)
14. K. Jedamzik, K.Y. Choi, L. Roszkowski, R. Ruiz de Austri, JCAP **0607**, 007 (2006)
15. J. Pradler, F.D. Steffen, Phys. Lett. B **648**, 224 (2007)
16. W. Buchmüller, L. Covi, K. Hamaguchi, A. Ibarra, T. Yanagida, JHEP **03**, 037 (2007)
17. A. Ibarra, arXiv:0710.2287 [hep-ph]
18. M.Y. Khlopov, A.D. Linde, Phys. Lett. B **138**, 265 (1984)
19. M. Bolz, A. Brandenburg, W. Buchmüller, Nucl. Phys. B **606**, 518 (2001)
20. J. Pradler, F.D. Steffen, Phys. Rev. D **75**, 023 509 (2007)
21. V.S. Rychkov, A. Strumia, Phys. Rev. D **75**, 075 011 (2007)
22. T. Asaka, K. Hamaguchi, K. Suzuki, Phys. Lett. B **490**, 136 (2000)
23. J.L. Feng, S. Su, F. Takayama, Phys. Rev. D **70**, 075 019 (2004)
24. M. Endo, F. Takahashi, T.T. Yanagida, Phys. Rev. D **76**, 083 509 (2007)
25. T. Asaka, S. Nakamura, M. Yamaguchi, Phys. Rev. D **74**, 023 520 (2006)
26. J.L. Diaz-Cruz, J.R. Ellis, K.A. Olive, Y. Santoso, JHEP **05**, 003 (2007)
27. Particle Data Group, W.M. Yao et al., J. Phys. G **33**, 1 (2006)
28. G. Belanger, F. Boudjema, A. Pukhov, A. Semenov, Comput. Phys. Commun. **149**, 103 (2002)

⁹ Note that the mass of the lighter stop is $m_{\tilde{t}_1} \simeq 0.7m_{\tilde{g}}$ in the considered $\tilde{\tau}$ NLSP regions with $m_h > 114.4$ GeV.

29. G. Belanger, F. Boudjema, A. Pukhov, A. Semenov, Comput. Phys. Commun. **174**, 577 (2006)
30. M. Kawasaki, K. Kohri, T. Moroi, Phys. Rev. D **71**, 083502 (2005)
31. R.H. Cyburt, J.R. Ellis, B.D. Fields, K.A. Olive, Phys. Rev. D **67**, 103521 (2003)
32. K. Jedamzik, Phys. Rev. D **74**, 103509 (2006)
33. F.D. Steffen, JCAP **0609**, 001 (2006)
34. F.D. Steffen, AIP Conf. Proc. **903**, 595 (2007)
35. W. Buchmüller, K. Hamaguchi, M. Ibe, T.T. Yanagida, Phys. Lett. B **643**, 124 (2006)
36. S. Kasuya, F. Takahashi, JCAP **0711**, 019 (2007)
37. G. Sigl, K. Jedamzik, D.N. Schramm, V.S. Berezinsky, Phys. Rev. D **52**, 6682 (1995)
38. K. Jedamzik, JCAP **0803**, 008 (2008)